Ben-Gurion University of the Negev
Faculty of Engineering Science
School of Electrical and Computer Engineering
Dept. of Electrical and Computer Engineering

Fourth Year Engineering Project

Final Report

Optimization of a controlled inductor

אופטימיזציה של סליל מבוקר

Project number:	**p-2023-087**
Students	**Yuval Tanny 313361602**
(name & ID):	**Nir Kave 205711922**
Supervisor:	**Prof. Ben-Yaakov Shmuel**
Submitting date:	**30.07.2023**

Optimization of a controlled inductor

Students Names: Tanny Yuval, Kave Nir

yuvaltan@post.bgu.ac.il

Advisor: Prof. Ben-Yaakov Shmuel

Abstract:

An inductor is an electrical component, with a certain amount of inductance, that stores energy. A controllable inductor (CI) is one whose inductance is controlled by an external DC current.

The purpose of this study is to present several guidelines for designing an optimal CI, given a set of requirements from the component.

It has been done by exploring the behavior of the electromagnetic fields and their influences on the inductance and magnetic losses.

In order to calculate these properties, we transformed the structures into magnetic circuits, and analyzed them (equivalently as electric circuits) using SPICE.

The second method we used is the Finite Element Analysis for mapping the magnetic behavior more accurately.

The Spice and the FEA analysis had shown that the greatest changes in the CI's behavior are coming from 3 parameters: windings, air gap and middle arm width.

There are several conclusions about the CI behavior in different structures that will be presented in a separate document that one could use to get guidelines for certain demands.

keywords: controllable inductor, optimal, electromagnetic, design, inductance, DC current.

<u>תקציר:</u>

סליל הוא רכיב אלקטרוני בעל מידת השראות, אשר אוגר אנרגיה. סליל מבוקר הוא סליל שאת השראותו ניתן לשנות על ידי זרם ישר.

מטרת מחקר זה הוא הצגת קווים מנחים לתכנון סליל מבוקר מיטבי עבור דרישות ספציפיות מהמכשיר.

על מנת להבין את הדרכים הטובות ביותר עבור תכנון של רכיבים מסוג זה, נדרש לחקור את הקשרים בין ביצועי הסליל המתוכנן, לבין המאפיינים הפיזיקליים שלו.

זה נעשה על ידי חקר ההתנהגות של השדות האלקטרומגנטיים והשפעותיהן על ההשראות ועל הפסדים מגנטיים.

שיטה ראשונה היא מידול מבנה הסליל למעגל חשמלי שקול בתוכנת "ספייס".

השיטה השנייה בה השתמשנו הייתה חקר דיפרנציאלי בעזרת שיטת "ניתוח האלמנטיים הסופיים" בעזרתה התבוננו בהתנהגות השדות האלקטרומגנטיים במבנים השונים.

שתי השיטות הראו לנו שהשינויים המשמעותיים ביותר בטווחי ההשראויות נעשים על ידי שינוי של 3 גורמים עיקריים: כריכות, מרווח אוויר ועובי הזרוע המרכזית.

ישנן מספר מסקנות מהתנהגות הסליל במבנים שונים אשר יוצגו במסמך נפרד, ממנו יוכל המתכנן לקבל קווים מנחים לפי דרישותיו.

מילות מפתח: סליל מבוקר, מיטבי, אלקטרומגנטיות, תכנון, השראות, זרם ישר.

Introduction:

Transformed and stored energy is a quality that is essential in many electronic circuits in the past few decades. There are several circuits that are commonly used, for example: DC-DC switched converters, Resonant Inverters, and Ballasts.

A main need in these circuits is a component that can store and release energy.

The inductor is a conductive wire helixed around a ferromagnetic core. When an electric current flows through the wire, it causes a magnetic flux inside the core. The ratio between the magnetic flux and the current is called Inductance (L).

The ability of this device to store energy is dependent on the value of its inductance.

Therefore, the use of reactive components such as the inductor, allows the designers to create circuits with much more efficiency in a manner of energy supply.

The controllable inductor is one whose inductance can be modified by using a direct current (DC).

To control the inductance, we can find a way to control the permeability (μ) of the inductor, which is the ratio between the magnetic flux density (B) and the magnetic field (H) that's creating it:

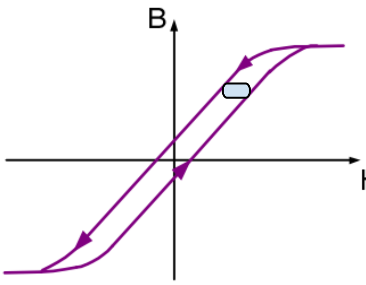

Fig. 1. B-H graph (Hysteresis).

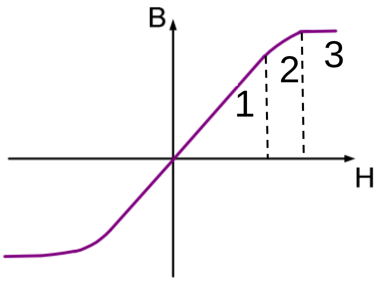

Fig. 2. Simplified B-H graph.

$$\mu = \frac{\partial B}{\partial H} \tag{1}$$

The permeability (μ) is the local slope of the simplified graph (Fig. 2). As it seems in Fig. 2, there are three main regions. In areas 1 (Linear) and 3 (Saturation), the permeability would stay constant, and thereby the inductance won't change. The changeable permeability would be in area 2. For a small variating signal (AC), the rate of change between B and H would stay approximately linear in a small area around a chosen point on the graph- operation point (OP).

It can be seen that for different OPs, we get a different slope which means different permeability that causes different inductance. In order to change the OP we need to change the H field with a bigger DC signal. That can be obtained by using another coil with DC current that will produce a constant magnetic field on the core and superposed with the AC magnetic field.

It's easy to see that the biggest μ value is at the area 1, where H field is lowest, since the slope is at its maximum in this area. The μ value is getting lower the more we are increasing the H field, meaning increasing the DC current (the B-I relation is in appendix A).

For summary, the inductance of the CI, which proportional to μ (the L-μ relation is in appendix A), is controlled by a DC current, with an opposite proportion.

Major problem in designing a CI is the fact that there is no “guide” for the optimal structure given the demands from the circuit.

Hence, the objective of this study is to create a spreadsheet that enables the construction of a CI based on specific requirements.

There are several ways to design this kind of inductor. One basic design is the following structure [1]:

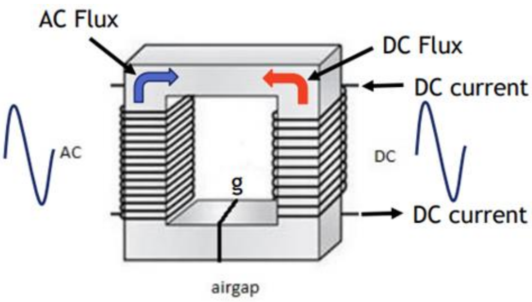

Fig. 3. Basic structure of controllable inductor [1].

With a changed DC current, the magnetic flux will be modified, which will cause the magnetic “conductance” (permeability) to change and to influence the inductance. That is how, indirectly, we can control the inductance by DC current.

Studies and research about the controlled inductor usually includes the presentation of a given CI that could work in a certain circuit, and analysing its operative properties that are relevant to this circuit. However, it appears that there is no ambition for making these CIs as optimal as they can be for their specific uses.

For example, for an LLC resonant converter with variable inductor [2], the article describes the inductor (Fig. 4), its properties and the role of each feature in it, but there is no consideration in the needs of the LLC for this specific design of inductor (‘double E-core’):

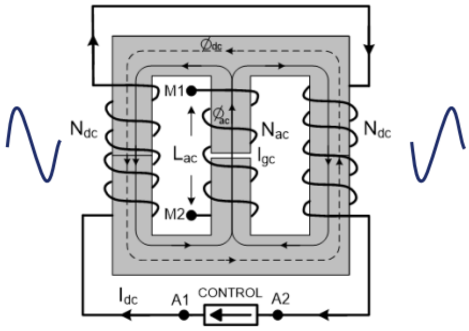

Fig. 4. ‘Double-E’ core [1].

Another example is a research that presents a variable inductor based bidirectional DC-DC converter [3], and a known structure of CI was picked with no optimization or adjustment.
In both cases, perhaps other structures would be more suitable for the circuit's requirements.
The ‘double E-core’ is an example of an improvement to the structure below (Fig. 5) in which a choke was added, in series to a regular core, which filter the DC current only:

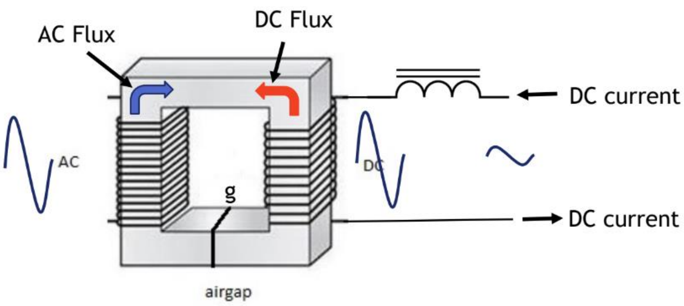

Fig. 5. Choke in series to basic controllable inductor [1].

The ‘double E-core’ reduces 3 problems: first, the coupling between the DC inductors to the AC inductor. second, the initial main inductance, and last, it reduces the amount of DC current needed. However, for this structure to perform a large range of inductances we need to reduce the air gap, which on the other hand causes a reduction of capability to carry heavy AC currents needed in resonant circuits [4]. Another problem is that the AC voltage between the two ports (A1;A2 in Fig. 4) is not 0 as ideally desired.
This approach, for instance, shows how to make a possible improvement for a certain kind of circuit, while for another system there could be a different solution that will be optimal.

To this day, no orderly process of synthesis was made to connect between optimal CIs structures, to different demands.

Every change we make can cause an advantage in one or more of the inductor's qualities, and from the other hand will impair other qualities.

Another type of losses that one must consider for getting an optimal operation of a CI, is magnetic losses. There are two main types we can discuss. First is the hysteresis loss which is caused by the change in the B field inside the core [5]. The amount of energy we are losing in any change of B can be approximated by measuring the area of the hysteresis graph created by this change (for example- the area marked on Fig. 1). The second loss is the proximity effect which is a parasitic capacitance created by magnetic forces between the winding of the wires [6]. These phenomenons can be approximated by certain assumptions, but for getting a much more precise analysis to a certain CI, one must calculate the magnetic losses in a numeric software (for example: Fig. 6).

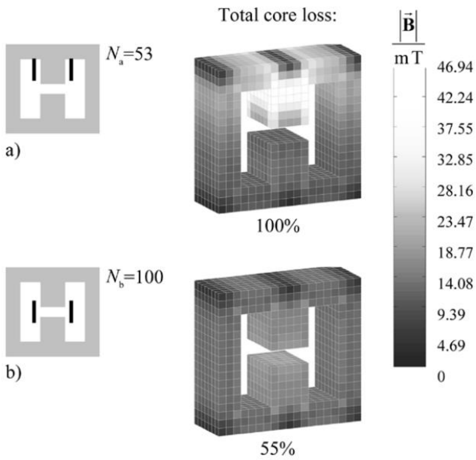

Fig. 6. Numeric calculation of magnetic core loss for two winding configurations [7].

Project Method:

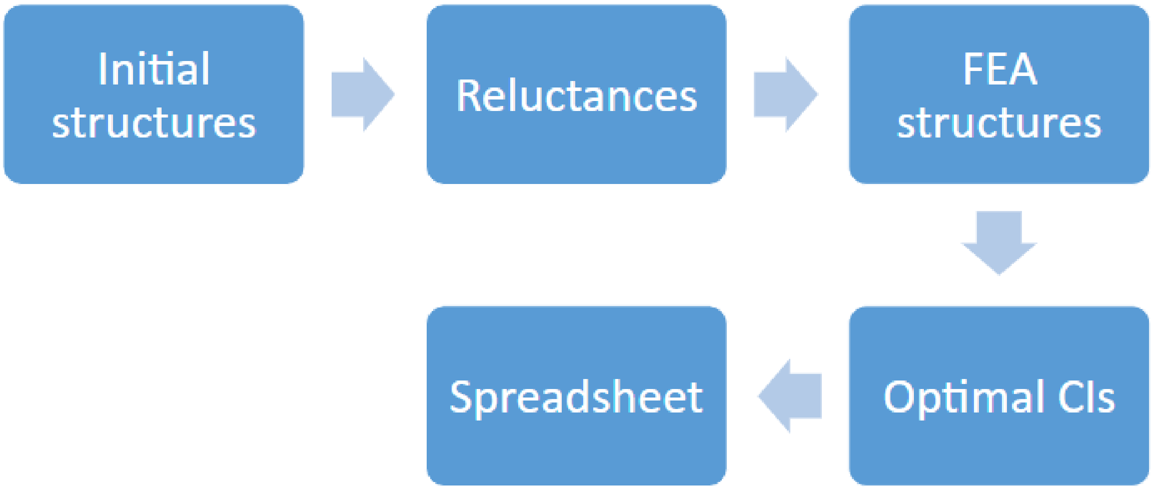

Fig. 7. Flowchart of the method we implemented.

Spreadsheet Planning:

Our product is a spreadsheet that is gathering the data collected from the results. In the spreadsheet, one can search his most suitable CI for his needs according to several parameters such as:

1. L-min
2. L-max
3. L-range
4. I-max
5. Resolution (Appendix B)
6. Hysteresis losses (for 10kHz, 100kHz, 1MHz)
7. Maximum magnetic energy waists in the air

Reluctance:

The first step of analysing the given structure and the influences of modifications over it, was to create an equivalent electrical circuit called reluctance. The whole process of design and simulation of the reluctance has been done using OrCAD platforms - schematic editor (Capture) and analog circuit simulation (PSpice), which gives us an approximate evaluation. The reluctance is a representation of the magnetic structure in which the components (resistors and voltage sources) and the electrical current represent the magnetic behavior of the CI.

Double E-core

In order to create the reluctances and measure the relevant parameters, we used several equations that were developed from an approximation of Ampere's law. Those equations are shown in Appendix C. The structure was converted to a schematic circuit as shown in Fig. 8:

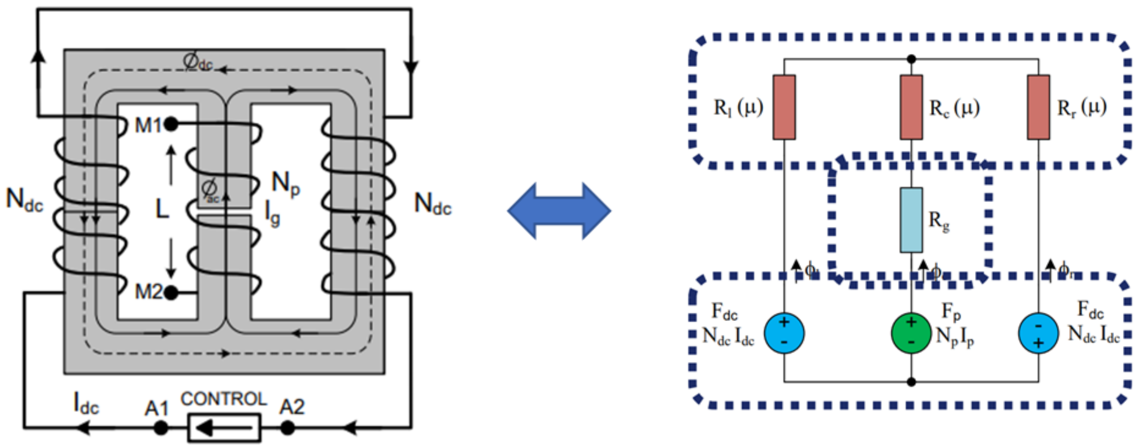

Fig. 8. Conversion of 'double E' core to an equivalent reluctance.

Fig. 9 is how the 'double E' core was implemented in OrCAD inspired by [8]:

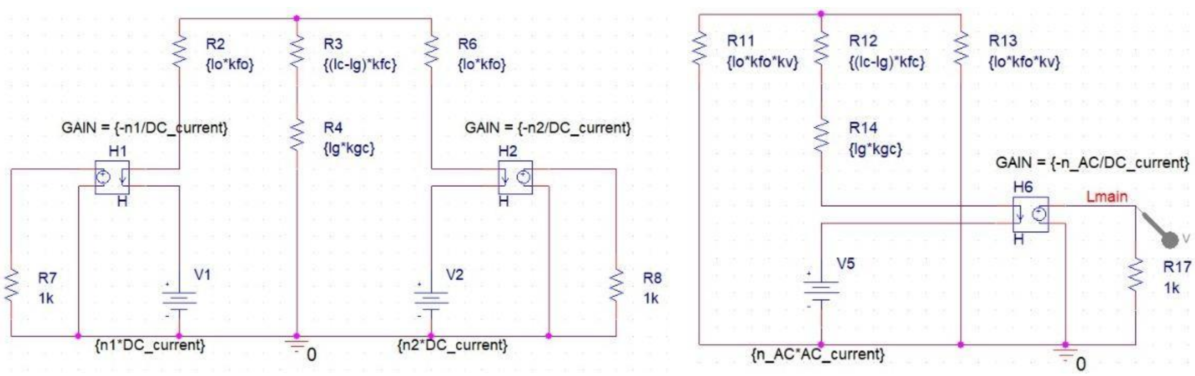

Fig. 9. The reluctance of 'double E' core in OrCAD separated into DC (left) and AC (right) equivalents.

The reluctance is a tool which can provide useful information to our needs, such as the range of inductance, fluxes etc. We concentrated at the inductance range of the AC coil.

The modified properties of the structure were:

1. Central arm's air gap.
2. Middle arm cross section.
3. Side arms cross section.
4. Number of windings.

Each property has 3 rates of values according to the table below:

	Air gap [mm]	Middle arm cross section [mm^2]	Side arms cross section [mm^2]	DC-windings
Small	0.2	$1.8^2 = 3.24$	$2^2 = 4$	15
Medium	0.5	$7.5^2 = 56.25$	$4^2 = 16$	45
Large	0.8	$12.3^2 = 151.29$	$6^2 = 36$	85

The simulations conducted as shown in [9], and each simulation was dedicated to modifying a single property of the list above, while the others are constant on medium scale, watching the plot of inductance over DC current, and documenting it for the conclusions part in the spreadsheet stage. Here, we assumed that the parameters are **independent**. The next stage (FEA) was to assume the opposite.

<u>Double Toroid core</u>

The same method was implemented on the double toroid. Now, the modified properties were:

1. Core's cross section.
2. Number of windings.

As for the double E core, 3 sizes for each property:

	Cross section [mm^2]	DC-windings
Small	$2^2 = 4$	15
Medium	$4^2 = 16$	45
Large	$8^2 = 64$	85

Results

An important concern that arises and is worth noting is the units of measurement resulting from the modeling process. For instance, the inductance is modulated by voltage which is represented by volts (V) (as you can see in Fig. 10) instead of henrys (H).

One of the four graphs we generated is presented in Fig. 10. It clearly depicts an L-"kv" curve, rather than an L-I curve. In this context, "kv" represents a parameter that directly modifies the permeability instead of the change in current itself causing it. This technique was taken from [9].

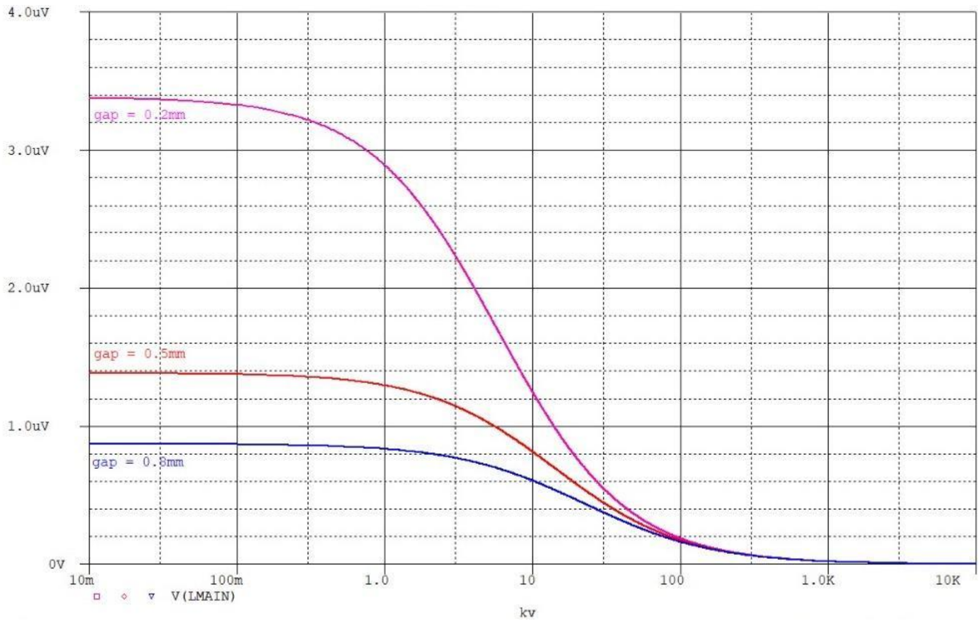

Fig. 10. L-”kv” curve for changing air gap.

We can see that the smaller the gap is, the range of inductance gets bigger up to maximum inductance value of 3.4uH in the structure with 0.2mm air gap.

FEA Analysis:

In order to get a better understanding of the electromagnetic behaviour of the CI, we used a Finite Element Analysis program.

The program we have used is “Femm”. Femm allows us to create any 2D structure we want, and it differentiates it to small and simple pieces and calculates the magnetic fields inside and outside.

Problems & Solutions

The main disadvantage of the program is that it doesn't have a DC sweep so we handled it with Lua scripting (Appendix D).

Method

At first, in order to get alined with the other groups of the CI projects, we chose to make our research with the 3C94 material as the core of the inductor (Fig. 11), Unfortunately, this material was too complex to analyse so we had chosen a “smoother” material in the manner of the B-H curve - N87 material (Fig. 12).

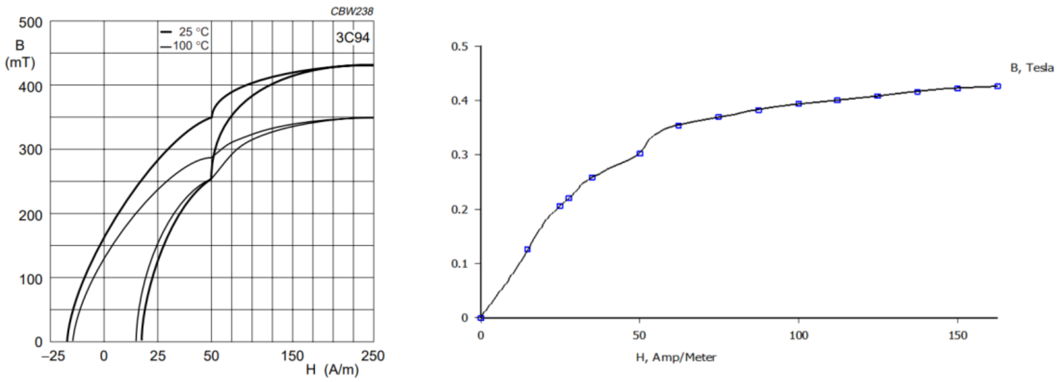

Fig. 11. B-H curve of 3C94 (left) [11], and its implementation in femm (right).

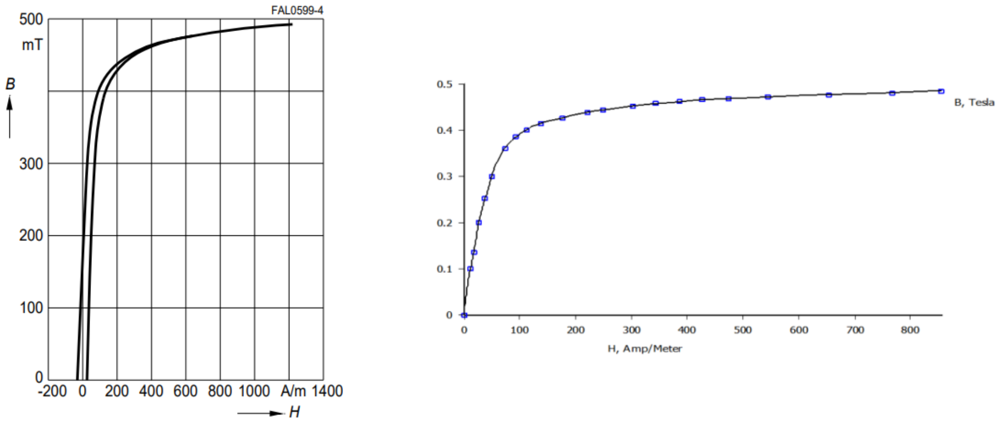

Fig. 12. B-H curve of N87 (left) [12], and its implementation in femm (right).

<u>Double E-core</u>

We have built the structure of the Double E-core according to a real CI we found in Power VI Seminar [1].

We wrote a Lua script that ran a DC-sweep current between 0-3 Ampere, through the winding in the side arms of the CI.

For every DC current, the program extracts the magnetic flux inside the middle arm, which has 10 windings coil around it with a constant current of 0.1 Ampere (Fig. 13).

The inductance is calculated in the script by definition- $L = \frac{Flux}{Current}$.

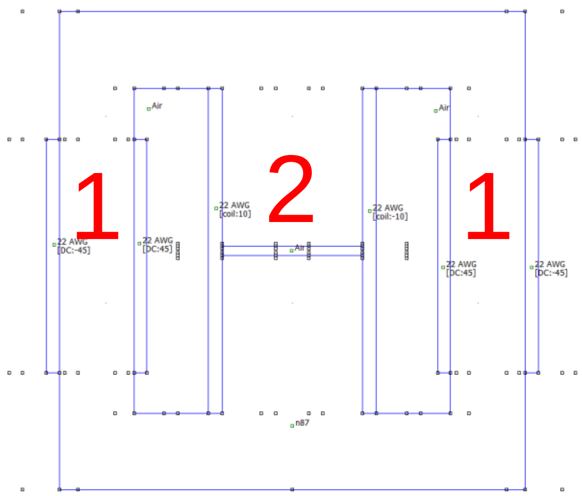

Fig. 13. Initial CI structure and windings (1- side arms, 2- main coil).

The changes we have made on the structure were:

1. Central arm's air gap.
2. Middle arm width.
3. Side arms width.
4. Number of windings.

Each modification has 3 rates of values according to the table below:

	Air gap [mm]	Middle arm width [mm]	Side arms width [mm]	DC-windings
Small	0.2	1.8	2	15
Medium	0.5	7.5	4	45
Large	0.8	12.3	6	85

With the assumption that these 4 variables may be **correlated**, we simulated all the possible inductors, meaning $3^4 = 81$ variations of the CI.

<u>Double Toroid core</u>

We implemented the same method on the double toroid structure.

We had built the initial structure according to the perimeter of the initial Double E-core (Fig. 14). This is because it's important to set the point of reference as the volume that the engineer can allow for implementation of the CI in his system.

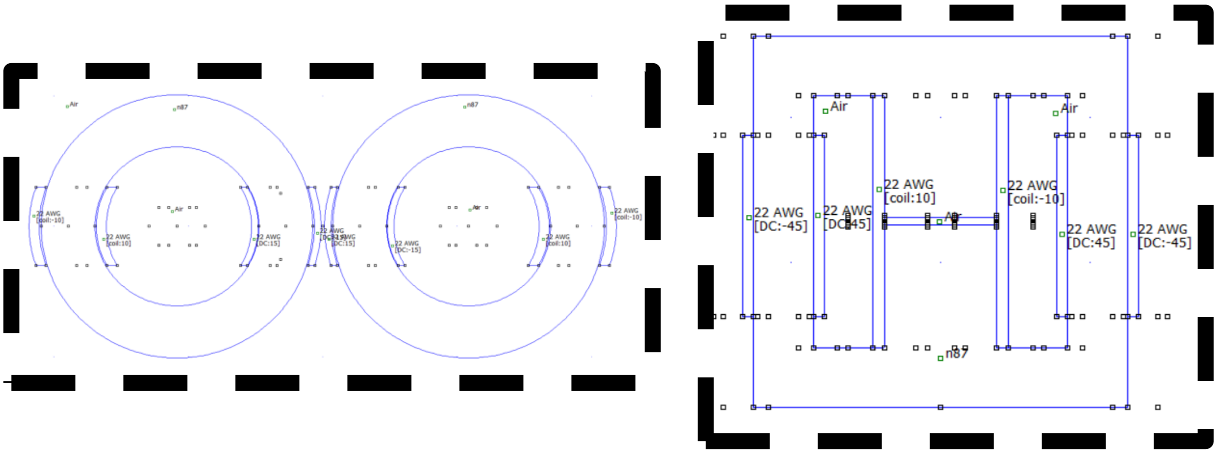

Fig. 14. General area of both CI.

For the double toroid we modified two different parameters which are: width of the ferrite and the DC windings, which means that there are 9 variations for this structure.

Same as in the double E core, each modification has 3 rates of values according to the table below:

	width [mm]	DC-windings
Small	2	15
Medium	4	45
Large	8	85

<u>Results</u>

For every variation we plotted The L-I curve, and for those that didn't get to saturation, we had expanded the DC sweep. For example in Fig. 15:

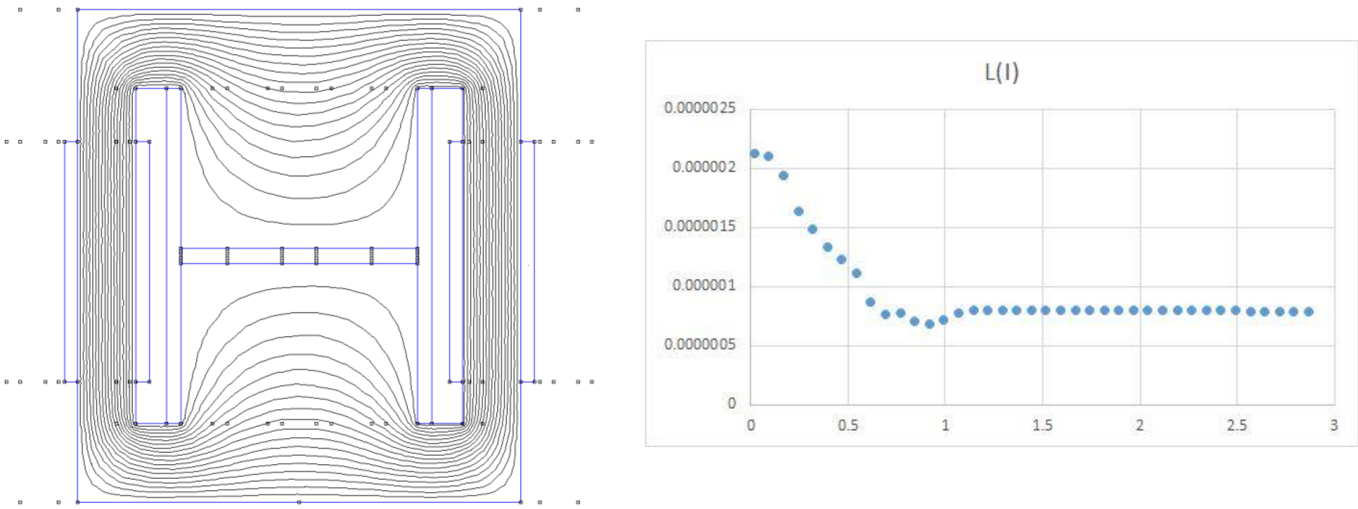

Fig. 15. Variation no. 13 (left): air gap (0.8mm), middle arm width (12.3mm), side arm width (2mm), DC windings (15) and its L-I curve (right).

To check if our method is valid, we implemented CI no. 13 in Spice (Fig. 16):

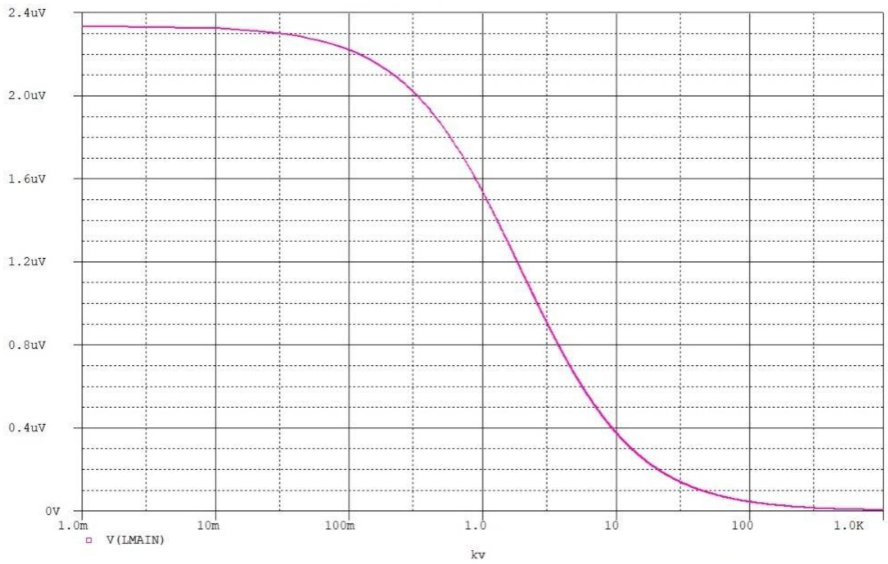

Fig. 16. L range of variation no. 13 in Spice.

The inductance range in both simulations is approximately similar.

Special modifications (Double-E core)

After we gathered all the 81 variations, we had decided to examine 3 more physical changes (Fig. 17). These changes were implemented on the best configuration in the manner of inductance (variation no. 10). The objective was to see if there is a more “elegant” way to improve the CI.

Change 1 and 2- “smooth corners”- the idea was to see what happens if we decrease the diffraction of the EM fields inside the ferrite.

Change 3 - since the magnetic flux lines inside the middle arm have a bow contour, we thought that change 3 (Fig. 17) can suit the CI.

We examine all the possible variations (7 combinations- 7 new structures).

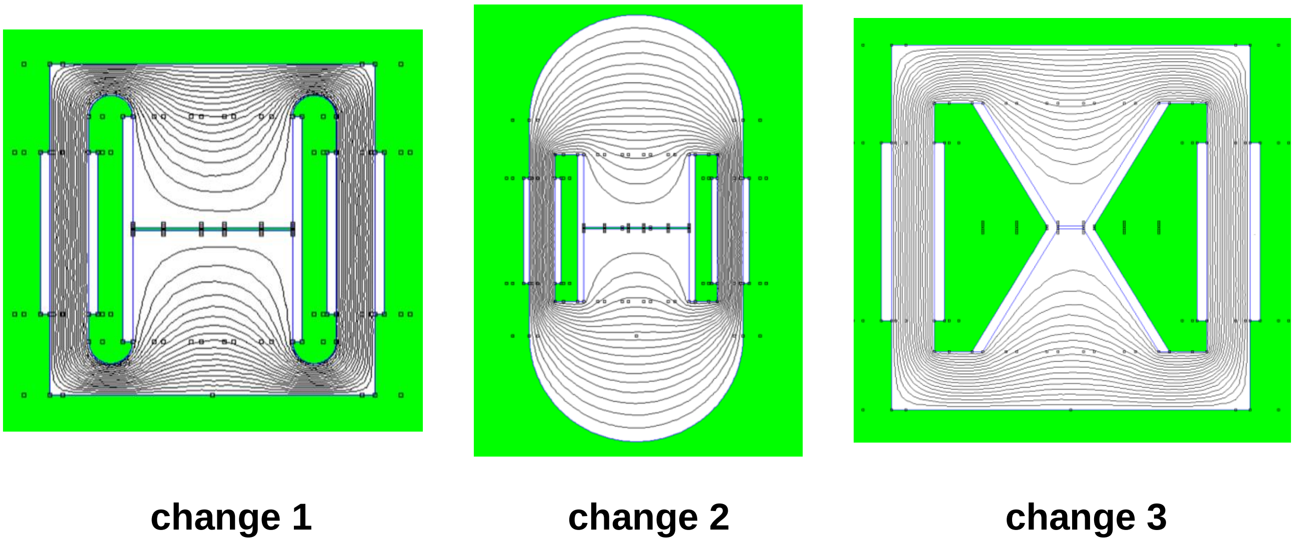

Fig. 17. Three types of changes- 7 combinations possible.

After analysis of the configurations, we compared them to the original variation (Fig. 18):

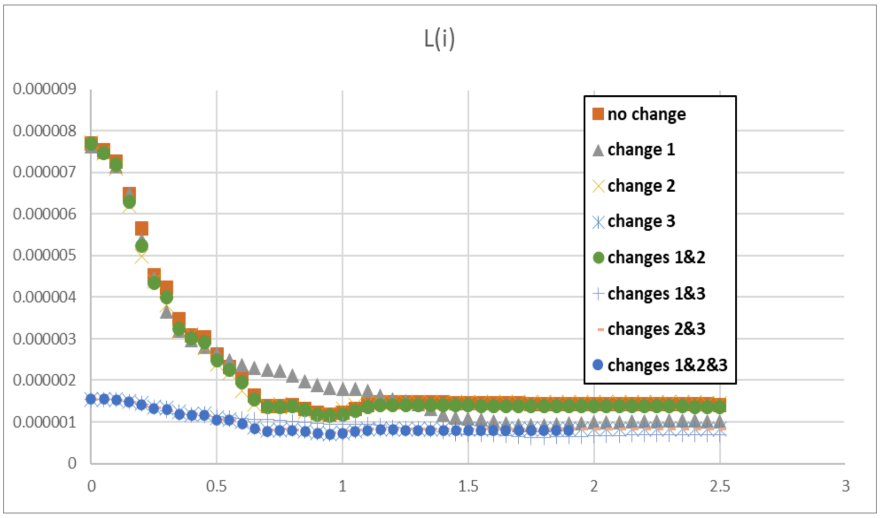

Fig. 18. L-I graph of the best CI and its special modifications.

CI's- "change 1", "change 2" and "change 1&2", were also added to the spreadsheet (10a, 10b, 10c respectively), due to their performance being nearly equivalent to CI no. 10, albeit with fewer losses.

Losses

For every variation we had extracted two different magnetic losses (Fig. 19):

-**<u>Hysteresis losses in the structure</u>**- for three rates of frequency (10kHz, 100kHz, 1MHz)

-**<u>Magnetic energy waste in the air</u>**- which can cause disturbances in the circuit that the CI is implemented to.

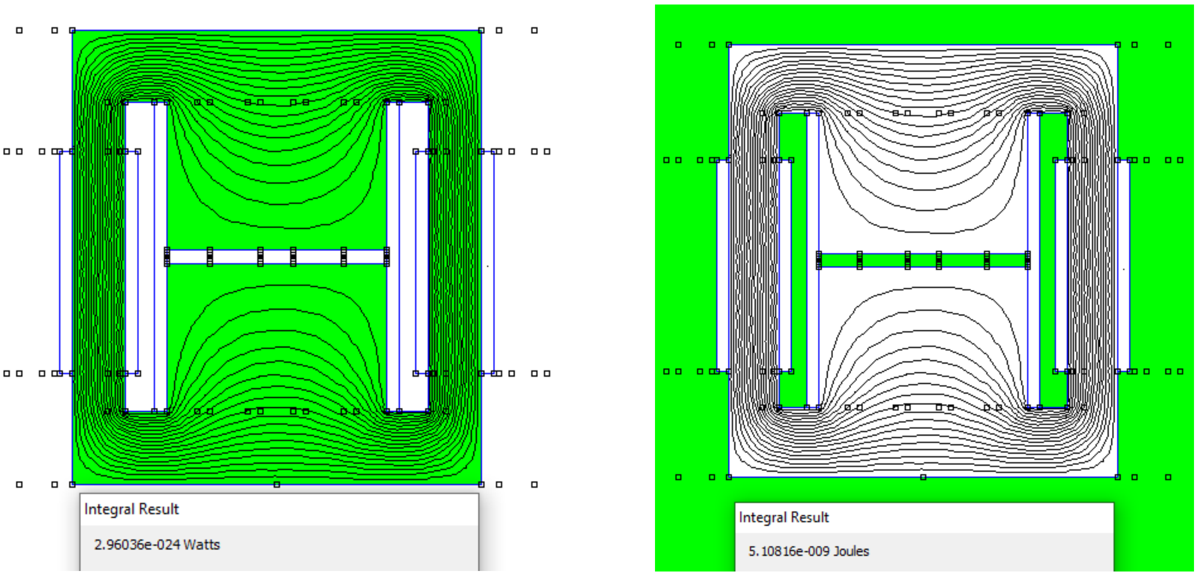

Fig. 19. Variation no. 13: Hysteresis losses inside the CI (left), magnetic energy waste in the air (right).

The results (Double E-core and the Double Toroid) were gathered in an excel table, from which we extracted our spreadsheet for the optimal CI.

Product Efficiency Rate:

In order to figure out the benefit of the spreadsheet, we calculated the rate of improvement/deterioration of the most/least recommended CI compared to a standard structure in every parameter separately. The standard structure was chosen to be an inductor in which all of the properties are medium according to what specified in the method section - which is core number 59 of the "double E" and core number 5 of the "double toroid".

The results of the "double E" core are presented here:

inductor number	parameter	increasing/decreasing times	increase/decrease
37	L min	370.37%	increase
81	L min	38.27%	decrease
37	L max	367.77%	increase
24	L max	23.22%	decrease
10	L range	507.69%	increase
31	L range	9.23%	decrease
76	I max	454.55%	increase
45, 42, 39	I max	20.20%	decrease
79	resolution	3006.38%	increase
39	resolution	5.25%	decrease
16	hysteresis losses (f=10kHz)	0.57%	decrease
18	hysteresis losses (f=10kHz)	483.98%	increase
10b	hysteresis losses (f=100kHz)	0.90%	decrease
39	hysteresis losses (f=100kHz)	785.74%	increase
49	hysteresis losses (f=1MHz)	0.21%	decrease
18	hysteresis losses (f=1MHz)	373.66%	increase

9	max wasted magnetic energy	6.67%	decrease
33	max wasted magnetic energy	1553.33%	increase

For example, we can see that inductor number 37 has an improved value of L-max by 3.67 of the standard structure. The results of "Double toroid" are presented in the spreadsheet.

Conclusions:

After we gathered all the data, we sorted the variations of the CI according to several parameters and concluded the following:

1. **Inductance range** - The inductance range was most influenced by two of the parameters which are:
   (a) The air gap- the best ranges were when the air gap was the smallest (0.2mm). The first 18 CI in the sorted data, were with this air gap.
   (b) The middle arm width- The first 9 of the CIs were with the widest middle arm.
2. **Resolution-** The resolution of the CI is **decreasing** with reduction of the air gap and incrementation of the middle arm width. In other words if we refer to conclusion no. 1, it means that the more you try getting a wider L-range, the less resolution you will have.
3. **Hysteresis losses** - Reducing the number of DC windings results in lower hysteresis losses.
4. In order to achieve minimum values of inductance, it is recommended to first build a relatively **narrow middle arm**.
5. **Special modifications of the Double E-core**- the three modifications (10a, 10b, 10c) have an improvement in the manner of hysteresis losses.
6. The double toroid structure has a range of inductances that is bigger in decades (100 times more) than the Double E-core.

Future work:

First, the next stage is to do the simulations with an FEA **3D** program. The program should support AC coil simulations to get a more complete picture about the whole device.

Second, if we want to expand the resolution and make the spreadsheet more accurate and with more options, we need to simulate more parameters such as:

1. Different ferrite materials.
2. Different conduction wires material.
3. Cross section of the wires.

Furthermore, we can also expand the rate for each parameter more than 3 sizes (S, M, L).
But of course, with every expansion, in manner of parameters or rate, the number of variations and simulations that needs to be done will increase exponentially.

Final Product- Spreadsheet:

After gathering all the data, we made a spreadsheet that its purpose is to allow the designer to decide what is better for him to implement in the manner of building the CI according to the demands from the inductor.

The spreadsheet:
https://docs.google.com/spreadsheets/d/1sZGhVD_R7Wefb8KhSS7C9pfKaNZBUAed/edit?usp=sharing&ouid=117174705847554648003&rtpof=true&sd=true

User manual video:
https://drive.google.com/file/d/1YPtfbawpQzIlOcODVQNv3FXrwApZ3502/view?usp=drive_link

References:

[1] Programa de Pós-Graduação em Engenharia Elétrica - UFSM. Variable Inductor Operation and Applications in Power Electronics. (Feb. 12, 2021). Accessed: Feb. 12, 2021. [Online Video]. Available: https://www.youtube.com/watch?v=J3HAtZwipoc

[2] Wei, Y., Luo, Q., Chen, J. and Alan Mantooth, H. (2020), Analysis and design of LLC resonant converter with variable magnetising inductance control. IET Power Electronics, 13: 3528-3536. https://doi.org/10.1049/iet-pel.2020.0007

[3] M. W. Beraki, J. P. F. Trovão, M. S. Perdigão and M. R. Dubois, "Variable Inductor Based Bidirectional DC–DC Converter for Electric Vehicles," in IEEE Transactions on Vehicular Technology, vol. 66, no. 10, pp. 8764-8772, Oct. 2017, doi: 10.1109/TVT.2017.2710262.

[4] D. Medini and S. Ben-Yaakov, "A current-controlled variable-inductor for high frequency resonant power circuits," Proceedings of 1994 IEEE Applied Power Electronics Conference and Exposition - ASPEC'94, 1994, pp. 219-225 vol.1, doi: 10.1109/APEC.1994.316396.

[5] Sam Ben-Yaakov, ElectronicBits#22 - HF Power Inductor Design (Oct. 26, 2016). Available: https://www.youtube.com/watch?v=6Mi8QDD71vE&t=2358s

[6] Mor M. Peretz, Ben Gurion University, Beer Sheva, Israel. DC-DC Converters. (Nov. 7, 2021). [Online Video]. Available: https://www.ee.bgu.ac.il/~smps/

[7] A. Stadler and M. Albach, "The influence of the winding layout on the core losses and the leakage inductance in high frequency transformers," in IEEE Transactions on Magnetics, vol. 42, no. 4, pp. 735-738, April 2006, doi: 10.1109/TMAG.2006.871383.

[8] Sam Ben-Yaakov, Magnetic Circuits And SPICE: A Practical Example: Part I Of Two Parts. (Nov. 22, 2022). Accessed: Jan 9, 2023. [online video]. Available: https://www.youtube.com/watch?v=JDgdT-gkqj4&t=829s

[9] Sam Ben-Yaakov, The Controlled Inductor And An LLC Converter Application Example. (Dec. 4, 2022). Accessed: Jan 9, 2023. [online video]. Available: https://www.youtube.com/watch?v=jmIdYymO7rE

[11] 3C94 Material specification, FERROXCUBE, Eindhoven, Netherlands, 2004.

[12] SIFERRIT material N87, TDK Electronics, Chuo City, Tokyo, Japan, 2023.

[13] Mikail Ansari. Design Automation (FEMM Scripting, Lua Scripting, Potential Artificial Intelligence AI Foundations). (Dec 30, 2022). Accessed: May 15, 2023. [Online Video].

Available:

https://www.youtube.com/watch?v=_RaFfaVb3tg&t=258s&ab_channel=MikailAnsari

Appendix A - variables and constants:

1. $B = \frac{n}{l} I$

   B - magnetic flux density

   n - number of wire turns around the core

   l - length of the core

   I - electric current

2. $L = \frac{n^2 A}{l} \mu$

   L - inductance

   n - number of wire turns around the core

   A - cross section area of the core

   l - length of the core

   μ - permeability

Appendix B- Resolution:

We defined the resolution as the ratio between the L-range and the I-range of a certain CI that is taken from 0 current, to the current that brings the CI to saturation* (Fig. 20):

$$resolution = \frac{dI}{dL}$$

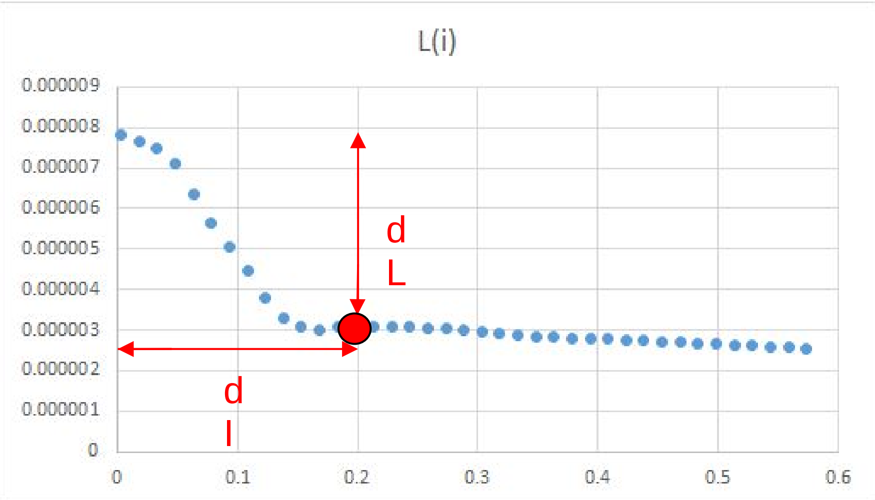

Fig. 20. Calculation of the resolution.

Meaning:

This ratio is giving (in an average approach) the idea of how it would be difficult to obtain specific inductance in the range. The more resolution you will have- the more accurate you can get with applying the wanted inductance.

*Note: to simplify the rate of resolution in the spreadsheet, we normalised the values in the spreadsheet by 10^4.

Appendix C- magnetic circuits or reluctance:

The reluctance model is a circuit that simulates the magnetic behavior of a certain structure. The figures in the reluctance are equivalent to a regular electric figures in the following form:

- F is the magnetic force, equivalent to electric voltage V.
- R is the magnetic resistance (reluctance), equivalent to electric resistance R (usually it marked as "$\Re$")
- ϕ is the magnetic flux, equivalent to electric current I.

These are defined by the following equations:

1. $F = nI$
2. $R = \frac{l}{\mu A}$
3. $\phi = \frac{F}{R}$

n - number of windings

I - electric current in the wire

l - length of the magnetic flux's path

μ - permeability of the the magnetic flux's path

A - cross section area of the magnetic flux's path

The reluctance of the air gap: $R_g = \frac{l}{\mu_0 v A}$

v- fringing factor - the magnetic flux in the air gap is spreading in the air (fringing). The v factor evaluates the loss of magnetic conductivity in this path (Fig. 21)

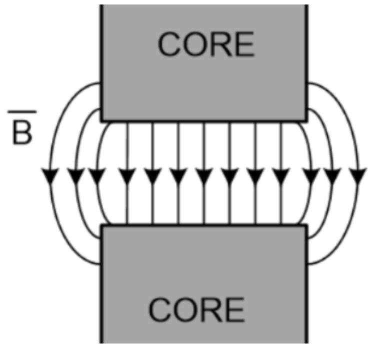

Fig. 21. Magnetic flux density in the air gap [1].

Appendix D- Lua Script:

The FEMM program can be used manually through its terminal. So for initial examinations and design, it is convenient to use this method.

Moreover, if one needs to run a series of simulations, the manual method is not practical to use, and it needs to be controlled by Lua scripting. Lua scripting is a programming language that has various functions that can control the FEMM program.

With coding the right script, one can do multiple simulations while changing parameters of the structure. For example (Fig. 22):

`open("DoubleE_core.FEM")`	Opens the femm project
`file1= openfile("LOSSES.xls", "w")`	Creates excel file to write the results
`mi_probdef(100000)`	Defines a 100kHz simulation
`mi_modifycircprop("DC", 1, 0.1)`	Defines the DC current to be 0.1 Ampere
`mi_analyze()`	Runs the simulation
`mi_loadsolution( )`	Opens the results window
`mo_groupselectblock(1)`	Defines the area that we want to integrate
`T=mo_blockintegral(3)`	Export the Hysteresis losses to variable T
`write(file1,format("%.30f",T),"\n")`	Saves T in the excel file
`closefile(file1)`	Closes the excel file

Fig. 22. Lua script that calculates the Hysteresis losses in the CI.

המלצת ציון לדו"ח מסכם

<u>אם יש צורך, לכל סטודנט/ית בנפרד</u>

מספר הפרויקט: P-20____-______

הפרויקט:

שם המנחה החיצוני:

שם המנחה מבית הספר:

שם הסטודנט/ית: ת.ז.:

%		חלש 55-64	בינוני 65-74	טוב 75-84	ט"מ 85-94	מצוין 95-100
20	הצגת גישת הפתרון, והתכנון ההנדסי					
20	הצגת התוצאות וניתוח השגיאות					
20	הסקת מסקנות					
10	גילוי יוזמה וחריצות					
20	פתרון בעיות, מקוריות ותרומה אישית (מעבר למילוי ההנחיות)					
10	עמידה בלו"ז ורמת הביצוע המעשי					

אם יש כוונה לפרסם/ יפורסם מאמר, שם כתב העת ומועד משוער להגשה:

ציין אם יש כוונה לשקול המלצה כפרויקט מצטיין:

הערות נוספות: